A 3D high-speed probe for measuring the magnetic components of a whistler wave

by

Pakorn Wongwaitayakornkul

A final report for SURF 2013

Mentor: Paul M. Bellan

Co-Mentor: Xiang Zhai

September 2013

Abstract

In the Caltech astrophysical jet experiment, observations show that a burst of wave activity in the whistler frequency regime (10-30 MHz) occurs at the time of a fast magnetic reconnection. The whistler wave magnetic component is expected to be circularly polarized even for oblique propagation and also contains most of the energy*. An inductive whistler wave detector has been designed using B-dot probes to measure the 3D high frequency magnetic field fluctuation. Each probe component consists of two miniature commercial oppositely oriented inductor coils connected to a miniature transformer. The transformer subtracts the signals of the two coils to cancel the unwanted capacitive component and retain the inductive component. The three coil pairs are arranged orthogonally and are adjacent to each other. The probe has excellent rejection of capacitive coupling and should resolve the whistler wave polarization. The measurements will be compared with other diagnostics, namely a capacitively coupled probe, an ultra-high-speed camera and a EUV detector.

* Bellan, P. M. (2013) *Circular polarization of obliquely propagating whistler wave magnetic field*. (submitted for publication)

Acknowledgement

I would like to thank Dr. Paul Bellan, my mentor, for providing me the opportunity to work under his direction this past summer. Also I would like to thank Xiang Zhai, my co-mentor, for helping me in every aspect of the project. I thank all members of Bellan research group for their insight and guidance. Finally, I wish to thank Caltech SURF program to financially support this project.

Table of Contents

1. Introduction

1.1 Background

Study of magnetic reconnection, the process by which magnetic field lines break and then reconnect to form a different topology, has been one of the most excited topics in plasma physics for decades [1-3]. It is believed that Hall magneto-hydrodynamics (HMHD), a MHD model with an extra term showing that magnetic flux is frozen into the electron fluid instead of the plasma center of mass, provides a pathway for magnetic reconnection that is prohibited in ideal MHD. In the Caltech astrophysical jet simulation experiment, a burst of wave activity was found in the whistler frequency regime by a capacitively coupled probe [4]. These waves are created at the location of magnetic reconnection and learning about these waves may reveal the mystery of magnetic reconnection.

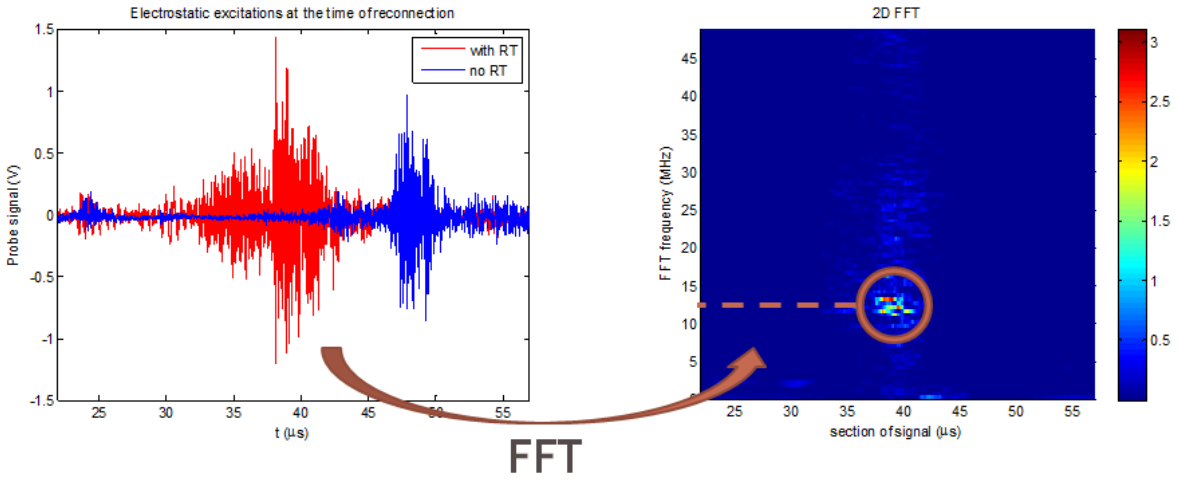

Figure 1: Electrostatic excitation at the time of magnetic reconnection suggesting the existence of whistler wave at around 13 MHz

Magnetic induction probes (B-dot probe) have been commonly used to diagnose plasma wave and other transiently induced fields since the 1960s [5-7]. The probe consists of loops of a wire. According to Faraday's law, a time varying magnetic field can drive a change in magnetic flux linked by the coil and thus produce a voltage across the coil terminals. In the past, many graduate students and post-docs of the Bellan group have used B-dot probes for detecting low frequency (≤ 1 MHz) magnetic fields created by Caltech's plasma [8-10]. The probe will be designed to measure whistler waves [11-12], high frequency phenomena generated during plasma jet experiment. The whistler wave generated in the plasma jet in Bellan lab has a typical frequency of 10-30 MHz and only exists for several microseconds. To measure the magnetic components of the high frequency wave, special techniques are required. Reilly et al [13] designed a probe for measuring plasma wave at

13.56 MHz, which is similar to the frequency of the whistler wave being considered [13]. Reilly includes explanations of how the probe works (reduction of capacitive pickup signal) and its characteristic frequency response. These explanations provide valuable information for designing a b-dot probe for whistler wave detection at Caltech.

1.2 Theory of magnetic induction probe

Faraday's law states that a time varying-magnetic flux of a loop of wire induces voltage across the wire. Therefore, the magnetic induction probe could be made by measuring induced voltage across two ends of the wire and convert it to magnetic field through Eq. 1.

$$V_i = -\frac{d\Phi_B}{dt} \tag{1}$$

If every coil has N turns with an area A, Eq. 1 becomes $V_i = -NA\frac{d\mathrm{B}}{dt}$. The voltage presented, however, tends to be non-ideal due to several factors that cause signal attenuation through impedance mismatch. A detailed analysis could be found in [7, 14]. The NA value could be found through a calibration with a Helmholtz coil.

The magnetic probe is commonly used to measure transient fields in laboratory plasma discharges. Because of its set up, the measured voltage

could come from two sources. The first source is the induced voltage from a time varying magnetic flux through the coils inside the probe as described above. The second source is a capacitive pickup of the coils due to a potential difference between the coils and the plasma. Figure 2a below illustrates the difference between two sources.

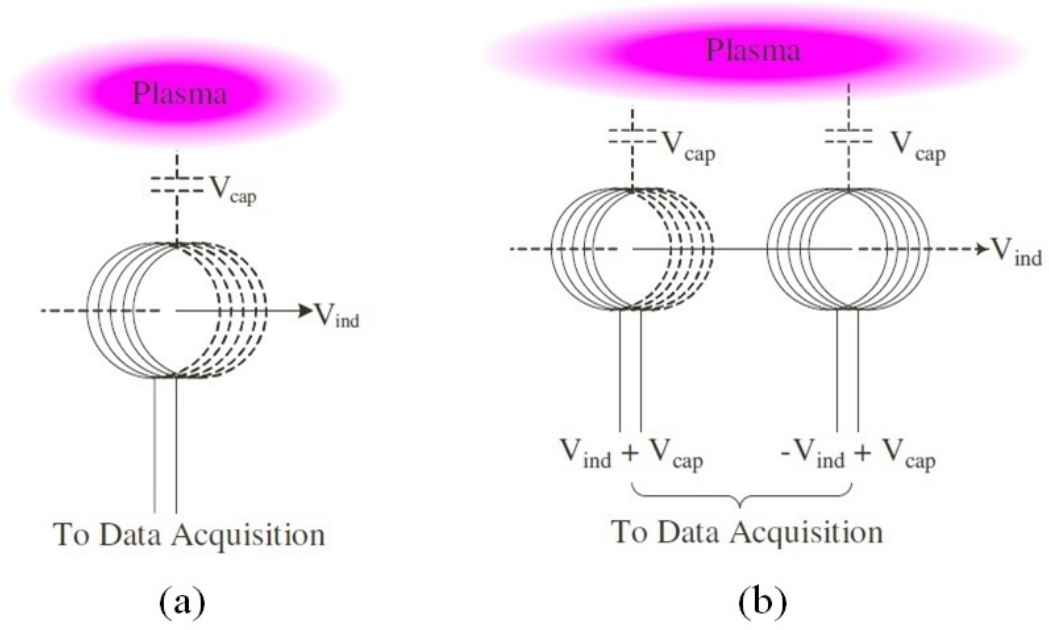

Figure 2: (a) Illustration of inductive and capacitive signals. (b) Two coils with opposite orientation [13]

Since the only signal of interest is the induced voltage from the time-varying magnetic flux, the unwanted capacitive pickup needs to be removed. This could be done by having two coils orientated 180° with respect to each other as shown in Figure 2b. Because the second coil is orientated in the opposite direction, the voltage pickup from time-varying magnetic flux across

the second coil is the negative of that across the first coil, while both coils pick up the same capacitive pickup voltages. The two signals can be subtracted through a center-tapped transformer to cancel the capacitive pickup signal.

2. Design and construction

The probe was designed and made. It should be able to resolve polarization of the magnetic component of the whistler wave at high frequency (up to 20 MHz). The capacitive coupled signal should be small comparing to the inductive one. The signal in each channel should be isolated (not interfere with each other). In this section, the design of the probe will be described. The order follows the signals' path, from where the magnetic field is measured to where the signals are eventually read out.

2.1 Inductor coils

Six commercial chip inductors with inductance 1 `H (@ 25 MHz) were used to measure magnetic field profile of three orthogonal orientations at one

location (Coilcraft Inc., model 1008CS-122). The dimensions of the chip are 2.8 mm x 2.9 mm x 2.0 mm. Figure 3 demonstrates the orientations of six chip inductors. In each orientation, two chips are attached to each other back to back to reduce the capacitive pickup signal as described in Section 1.2. Then commercial super glue is used to attach all three orientations together. They are mounted as in Figure 3b so that the probe can measure the magnetic field as close to the same location as possible. The signals will be sent through twisted wires (MWS MULTIFILAR, gauge 34 wires). The twisted wires are used to minimize the effective area of a close loop created from the wiring. The area can inductively coupled with the plasma discharge and cause the probe to pick up an undesirable signal. The whole parts are not exposed to the vacuum. They are covered with quartz tube.

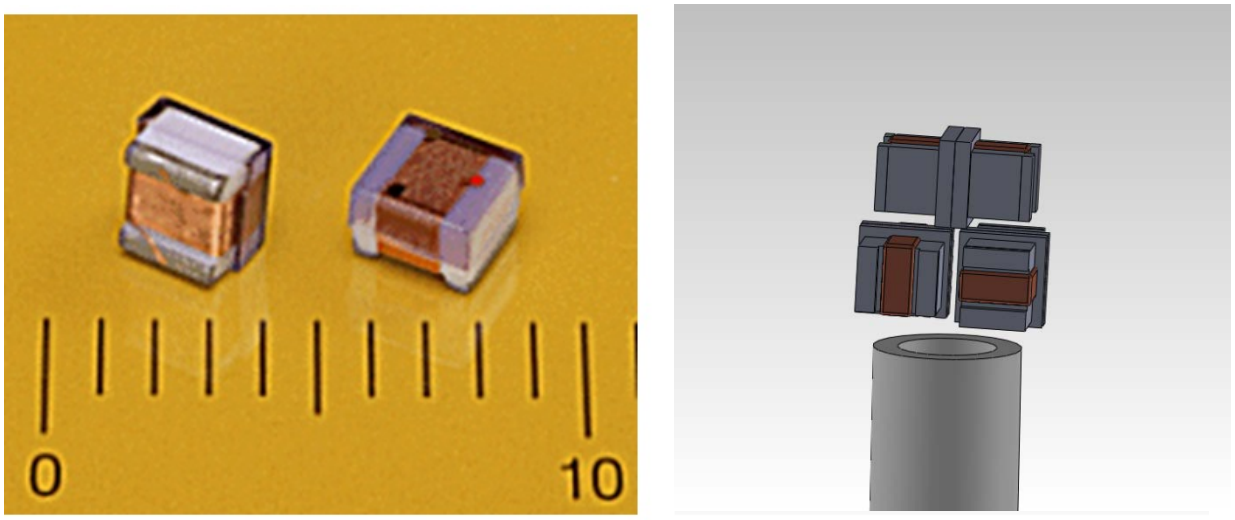

Figure 3: (a) Photo of inductor coils with dimension indicator. (b) Illustration of six inductors glued together orientated in three orthogonal components

2.2 Shielding with plastic retention

The signals are carried with several small wires. At high frequency ($f > 10\,\mathrm{MHz}$), there can be interferences between each channel. Therefore, Aluminum foil is used to separate each channel. The aluminum foil also acts as a shielding to block the wire to capacitively couple with the plasma. The wires go through a plastic retention tube. The tube is also shield with copper tape and electrical tape as shown in a figure below. The pattern of wrapping is to prevent any close loop at the location near the probe. All the shielding are connected to a common ground.

Figure 4: (top) schematic of copper tape wrapping around the plastic retention. (bottom) aluminum foil sheildig separating each wire

2.3 Transformer and circuit board

After going through the plastic retention, the wires are connected to a circuit board. The signals are subtracted through a 1:1 transformer (as explained in section 1.2). The result signals are connected to a USB connector. The system is designed so as to fit in a 3/4" stainless steel tube. The USB port consists of 4 pins: 3 for each channel and 1 for ground.

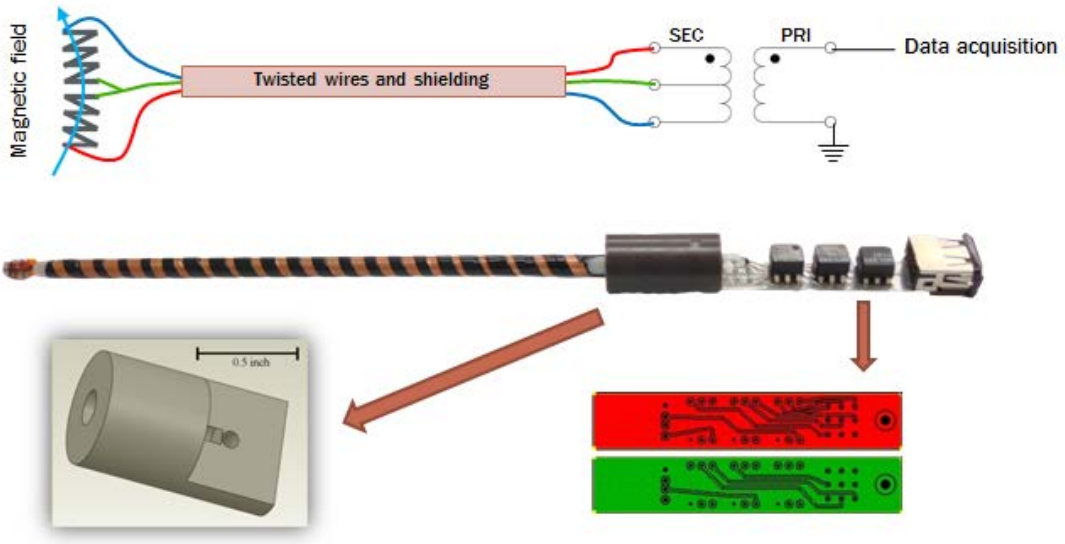

Figure 5: A diagram shows how signals are carried out and subtracted through transformer

2.4 Transmission lines

Originally, USB cable was chosen to carry the signal out of the chamber. However, at high frequency, there are large interferences between each channel. As a result, a USB to coaxial connector is made. Each coaxial carry the signal connected to the common ground. The signals then can be

read from connecting the BNC connectors to either oscilloscope or VME digitizer.

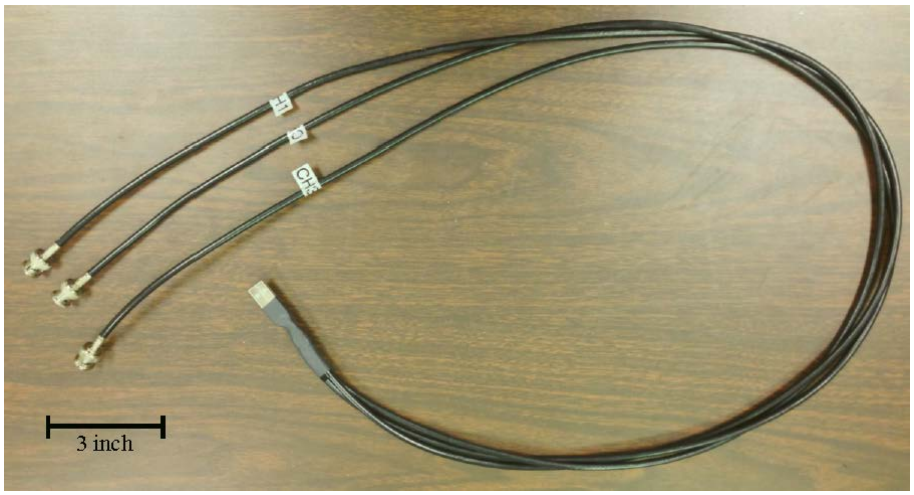

Figure 6: Image of the USB to VME digitizer

3. Result

3.1 Calibration

3.1.1 Operational principle

Previous work has shown that there are typically three ways to calibrate a magnetic probe [8]:

(i) Direct geometrical inspection of the coil dimensions (count n, measure A)

(ii) Measuring the output voltage when the coil is put in a known pulsed field

(iii) Comparison of the probe output with that of a coil of known dimensions, i.e., a Helmholtz coil and calculate what B should be generated compared to what B is measured.

Method (iii) has been found to be preferred method among these authors. It is also the technique that was used to calibrate magnetic probe array at Caltech in the past [8-10].

Using Faraday's law, the probe measures time-varying magnetic field by detecting the voltages across each coil. In each orientation (two coils),

$$V_{\text{coil}} = -\frac{d\Phi}{dt} = -2NA\left(\frac{dB_{\text{measure}}}{dt}\right)$$

$$B_{\text{measure}} = \frac{1}{-2NA}\int V_{\text{coil}}dt \quad \text{(2)}$$

where N is the number of turns in the coil and A is the area of the coil. The factor 2 appears in the equation corresponding to two coils used for the probe in each orientation. The probe can be calibrated using a known magnetic field generated from a Helmholtz coil. For a spatially designed and constructed Helmholtz coil with n turns of radius a, through which a current $I/2$ runs (current I generated from the generator through two wires, one on

each side of the Helmholtz coil, that connect in parallel), the magnetic field in the center is

$$B_{\text{applied}} = \left(\frac{4}{5}\right)^{3/2} \frac{\mu_0 nI}{a}$$

$$B_{\text{applied}} = \left(\frac{4}{5}\right)^{3/2} \frac{\mu_0 n}{2aL_H} \int V_{\text{H}} dt \quad \text{(3)}$$

where V_{H} and L_H are the voltage across and the inductance of the Helmholtz coil. Equating B_{measure} and B_{applied} gives:

$$NA = -\left(\frac{5}{4}\right)^{3/2} \frac{aL_H}{\mu_0 n} \frac{\int V_{\text{coil}} dt}{\int V_{\text{H}} dt}$$

In a perfect situation, the coils can be aligned in r, θ, and z and this calibration factor NA can be measured for each orientation. However, due to misalignment, there could be a pick up signal that is measurable in θ and z direction, although the probe is aligned in r direction.

In her thesis, Auna introduced a 3-by-3 calibration constant matrix $\mathbb{M}$ to correctly measure the magnetic field. Matrix $\mathbb{M}$ relates the applied magnetic field at the probe to the integral of the voltage across the coils through $\vec{\text{B}}_{\text{applied}} = \mathbb{M}\vec{A}$, where $\vec{\text{B}}_{\text{applied}}$ is the magnetic field in r, θ, and z,

and $\vec{A}$ is defined as $\vec{A} = \begin{pmatrix} \int V_{\text{coil,r}} dt \\ \int V_{\text{coil},\theta} dt \\ \int V_{\text{coil,z}} dt \end{pmatrix}$. By applying a magnetic field along a direction (r, θ, or z) and measure the voltages across each coil, each elements of $\mathbb{M}$ can be determined. Following this method, the expression for $\mathbb{M}^{-1}$ is

$$\mathbb{M}_{i,j}^{-1} = 2\left(\frac{5}{4}\right)^{3/2} \frac{aL_H}{\mu_0 n} \left(\frac{\int_{t_1}^{t_2} V_i^j dt}{\int_{t_1}^{t_2} V_{\text{H},j} dt} \right)_{i,j=\{r,\theta,z\}} \quad \text{(4)}$$

where i and j represent indices for rows and columns of the matrix $\mathbb{M}$ respectively ($\{1,2,3\} = \{r, \theta, z\}$). V_i^j represents the voltage across the coils oriented in i direction when measuring the magnetic field applying in j direction. $V_{\text{H},j}$ represents the voltage across the Helmholtz coil when applying the magnetic field in j direction.

However, integration acts as a low-pass filter and can kill off high frequency signal, which is what we want to detect. During the calibration, a sinusoidal wave at angular frequency ω can be chosen as the input voltage across the Helmholtz coils. Consequently, the voltages measured across the miniature coils are also sinusoidal at the same frequency. Therefore, we will use a relation $\vec{\text{B}}_{\text{applied,0}} = \mathbb{C}(\omega)\vec{V}_0$, where $\mathbb{C}(\omega)$ is a frequency-dependent

calibration matrix, $\vec{V}_0$ is a vector consisting of amplitudes of the sinusoidal voltage being measured across the probe (three elements; one for each orientation), and $\vec{\mathrm{B}}_{\mathrm{applied},0}$ is the amplitudes of the applied magnetic field in each orientation. In practical when the probe is used in the plasma chamber to observe whistler wave, one could perform a spectral analysis via Fourier transform on the signal to select a specific frequency to analyze. This way, the magnetic field can be found without integrating the voltage signals. Assuming $V_i^j = V_{i,0}^j e^{i\omega t}$ and $V_{\mathrm{H},j} = V_{\mathrm{H},j,0} e^{i\omega t}$, a similar derivation to Eq. (4) can be applied to $\mathbb{C}(\omega)$.

$$\mathbb{C}(\omega)_{i,j}^{-1} = 2\omega \left(\frac{5}{4}\right)^{3/2} \frac{aL_H}{\mu_0 n} \left(\frac{V_{i,0}^j}{V_{\mathrm{H},j,0}}\right)_{i,j=\{r,\theta,z\}} \quad (5)$$

3.1.2 Result of the calibration

B-dot probe is calibrated with the Helmholtz coil made by A. Moser [5]. A 20-MHz function generator (Wavetek, model 143) and digital phosphor oscilloscope (Tektonic DPO4104B) are used. A mini-circuit T1-6T RF transformers is again used as 1:1 transformer between the Helmholtz coil and function generator. The transformer is used to prevent Helmholtz coil from having a ground, which could result in a large background signal. The setup is shown in Figure 7.

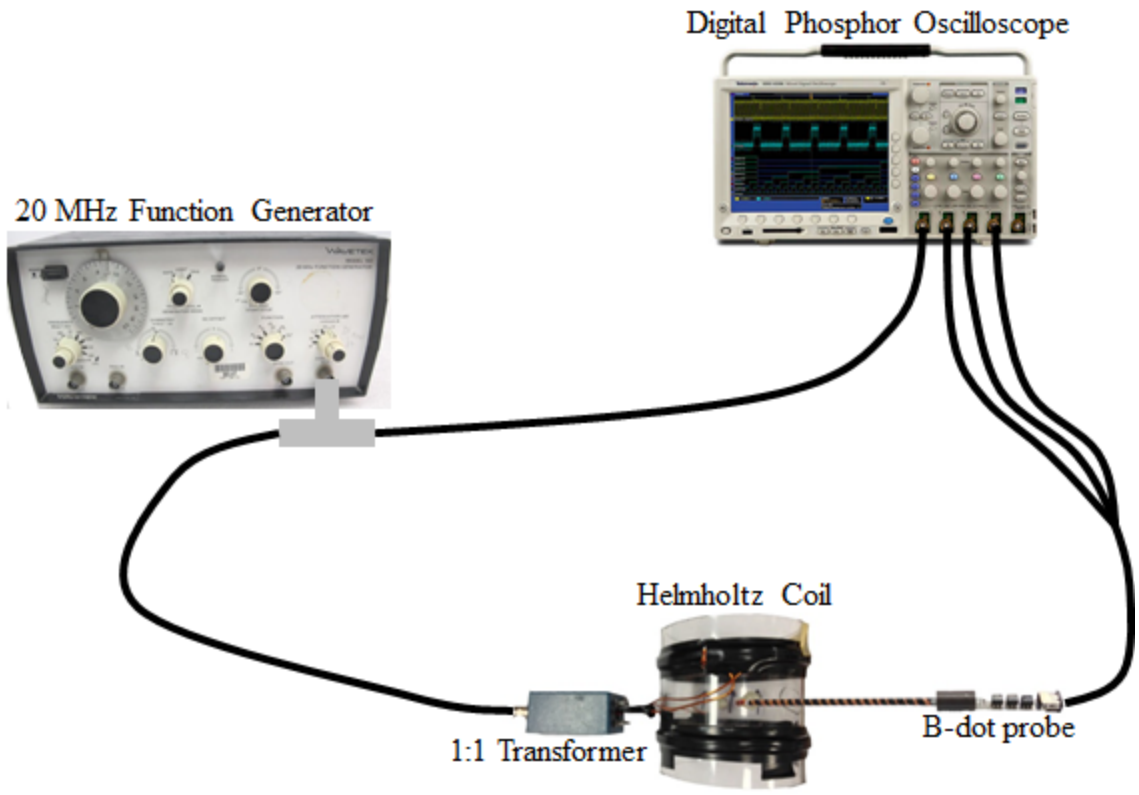

Figure 7: Diagram describes the experimental setup of the calibration (the image is not correctly scaled)

The output voltages can be measured from the channels 2-4 of the oscilloscope that connects directly to the probe. The input signal, however, is not quite the same as the voltage being measured from channel 1 of the oscilloscope. The actual input signal that runs through the Helmholtz coil can be deduced from the voltage across channel 1 of the oscilloscope multiplying by a frequency-dependent factor. The ratio is defined as a fraction of the amplitude of the signal measured after the transformer and at the function generator. This input voltage is calibrated and Figure 8 shows how this ratio varies with frequency.

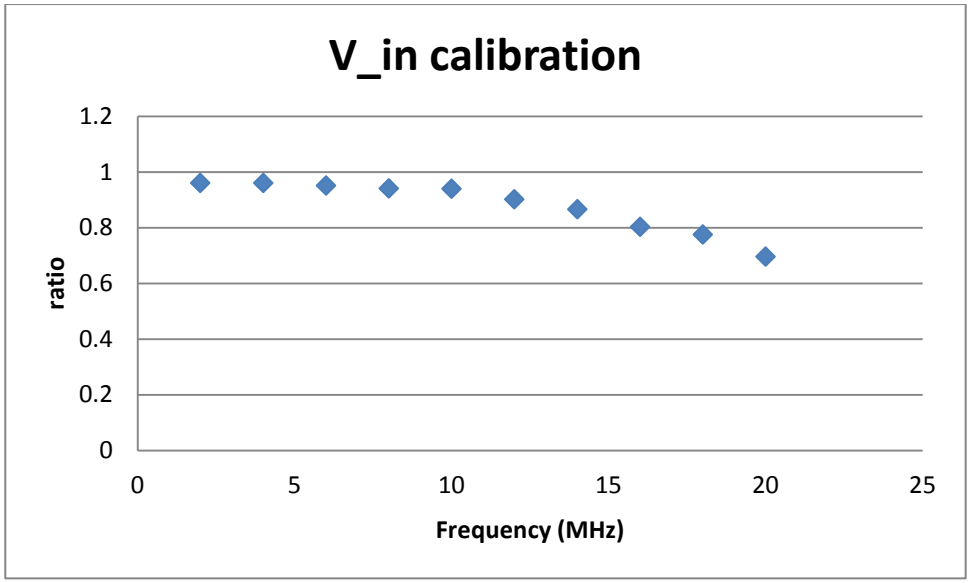

Figure 8: Graph shows how the ratio varies in frequency

We are now ready to perform the bench-test calibration. According to Eq. 4, $\mathbb{C}(\omega)^{-1}$ can be determined through finding $\frac{V_{i,0}^{j}}{V_{\mathrm{H},j,0}}$ for each i and j. However, instead of using the ratio of the amplitude of output and input signal, which uses only the peaks of the data, we can plot a graph between input and output signal and then find the slope of such graph. With this method, we will be able to use all the points in the data. There could be some phase shifts between two signals due to an impedance mismatch. But we can manually shift two signals to be in phase. The measurement is performed at 11 different frequencies: 1, 2, 4, 6, 8, 10, 12, 14, 16, 18, and 20 MHz. Figure 9 shows the result of the measurement. There are 3x11 plots in Figure 9. The measurements were taken at the same orientation in each row and same frequency in each column. Blue, magenta, and green correspond to

channel one, two and three. The signals show opposite orientations at around 11 MHz due to a large phase shift; therefore, in the last 4-5 columns, the slope of the signals has opposite sign from that in the earlier columns.

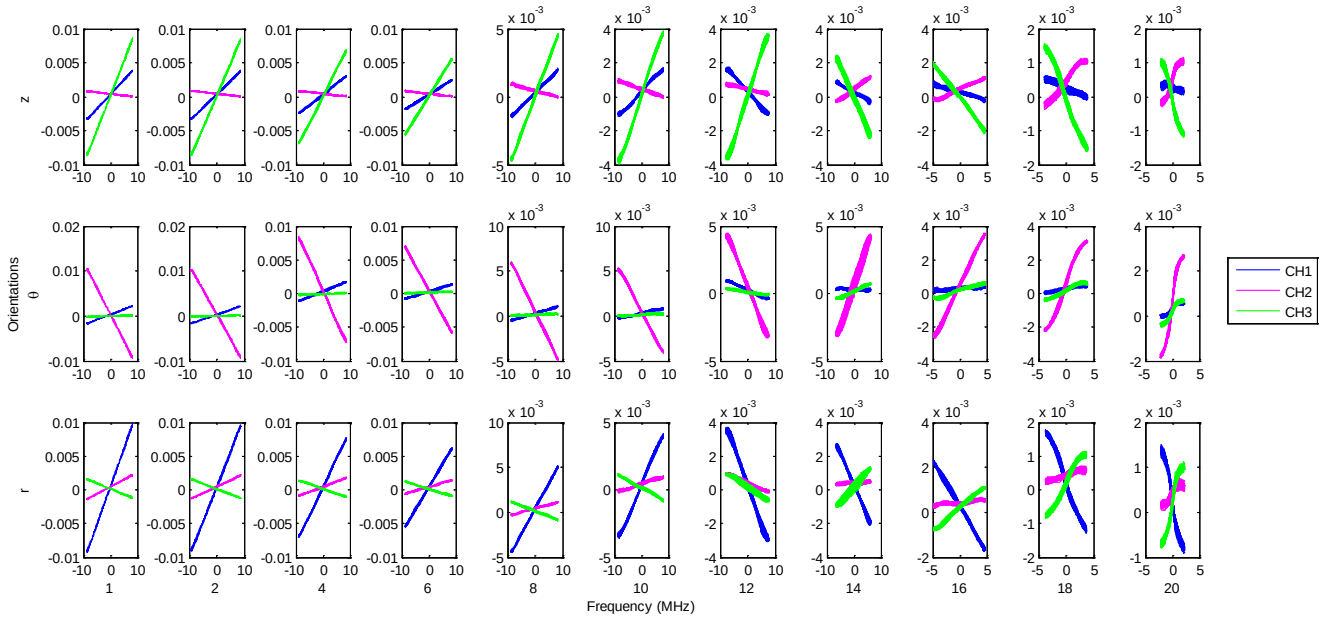

Figure 9: Plots of input (x) versus output (y) signals for three channels at different orientation and frequency

After the slope of each channel was determined at each frequency, the calibration matrix $\mathbb{C}(\omega)$ can be found. To visualize how each element of the calibration matrix progresses through the change of frequency, each element of the 3x3 matrix is plotted versus frequency in a 3x3 subplot style as shown in Figure 7. X-axes are frequency in MHz, while Y-axes are elements of $\mathbb{C}(\omega)$ in $\mathrm{m}^{-2}\mathrm{s}^{-1}$. To check its validity, we try to predict how these curves should

behave. According to Eq. 1, we can substitute $V_{\text{coil}} = V_{\text{coil},0}e^{i\omega t}$. Therefore, in a perfect situation where the coils are perfectly aligned with the orientations measured (r, θ, and z), $\mathbb{C}(\omega)$ should be a diagonal matrix and its diagonal element should be $c_{ii}(\omega) = -\frac{1}{2NA\omega}$, for i =1, 2 and 3. For comparison, this ideal case is also plotted in red in each of the diagonal element.

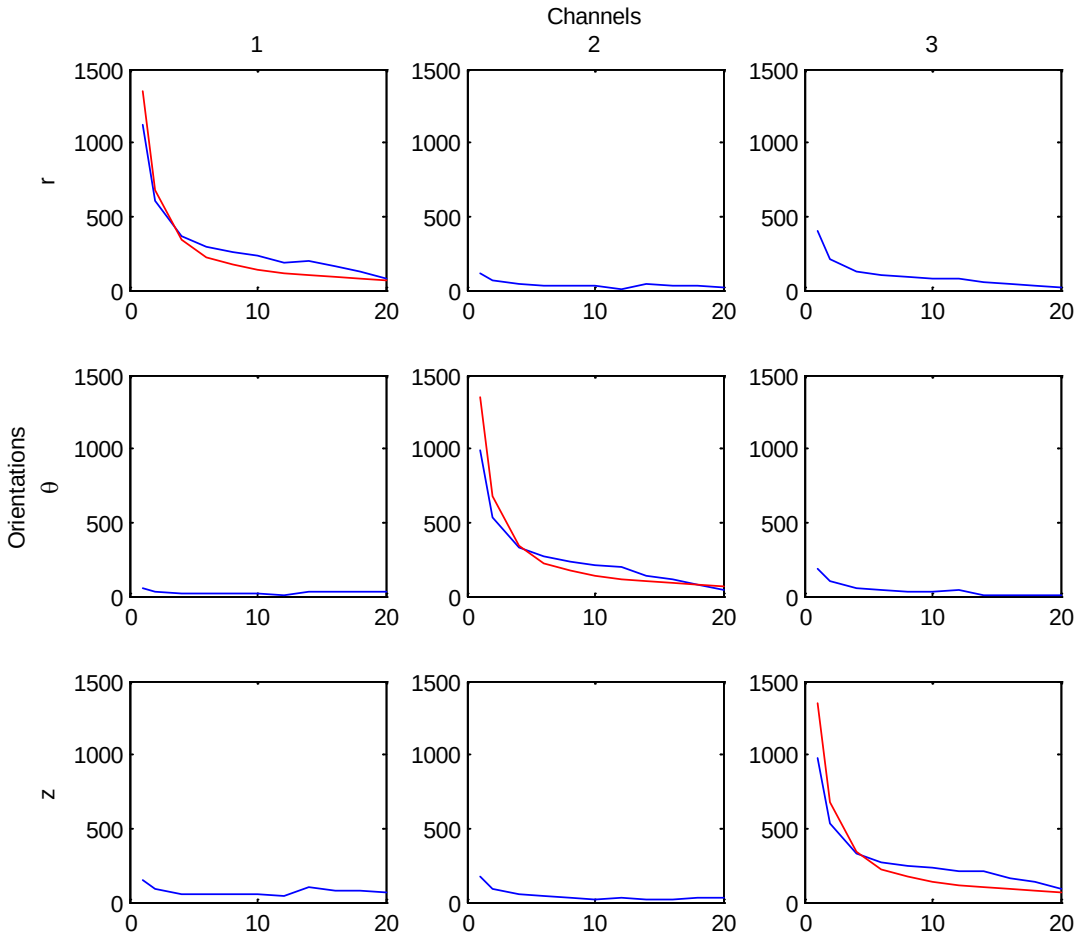

Figure 10: Plot of each element in calibration matrix at different frequency (blue) and its predicted value (red)

After calibration, the probe was installed to the plasma chamber. The capacitive coupling probe was also place close to our magnetic probe (whistler probe) to confirm the existence of the whistler wave. Several plasma shot were produced and measured. All the shots were taken from Argon plasma. Argon was chosen as it was heavy and expected to produce the largest signals. In the first two shots, only capacitor bank was used to ignite to plasma, while in the last shot, pulse forming network (PFN) was also used to increase the chance of magnetic reconnection. The signals of the whistler probe here are measured in Volt. They can be converted to magnetic field using the calibration matrix from Section 3.12.

3.2 Plasma shot

In the first shot, the signals from every channel are excited at the same time. A further investigation suggests that all the signals are in phase. In all the channels, excitations of wave at around 5 and 10 MHz were found.

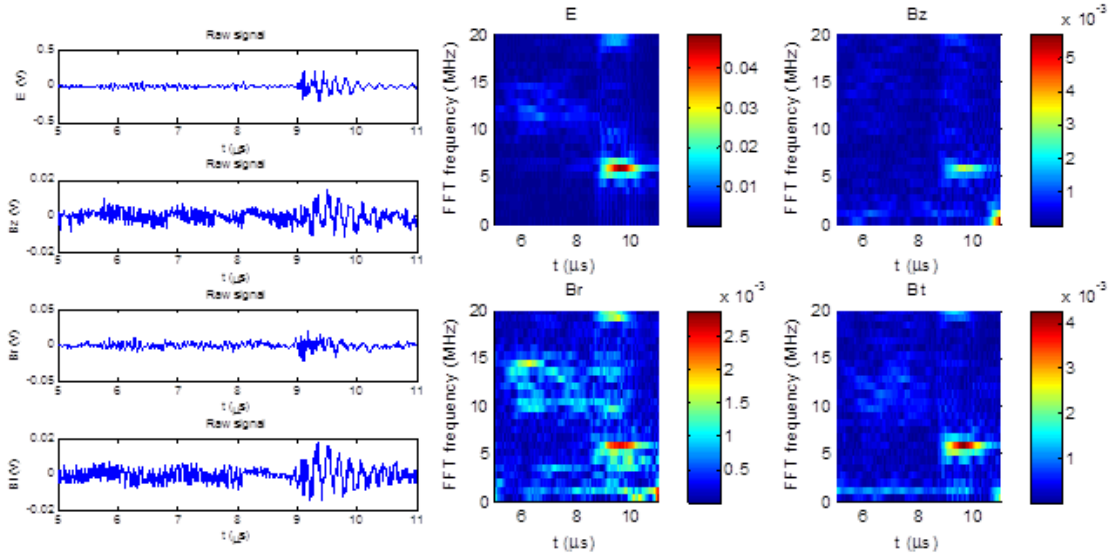

Figure 11: Shot #15136, CB only, All E and B are in phase. (left) plot of the signals over time for capacitive coupling probe and each of the channel of the whistler probe (right) the FFT of the graph on the left

Similarly, there was an excitation at around 5 MHz in the second shot. However, the magnetic component in radial direction (direction parallel to the probe) is 90 degree behind the other two.

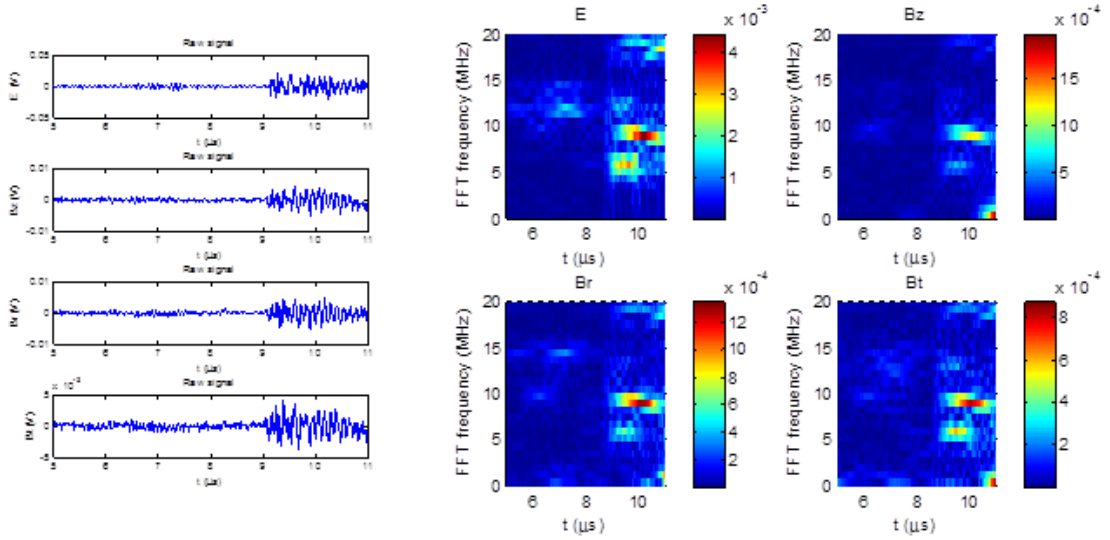

Figure 12: Shot #15140, CB only, Br is 90 degree behind other Bz and Bt. (left) plot of the signals over time for capacitive coupling probe and each of the channel of the whistler probe (right) the FFT of the graph on the left

Ultimately, pulse forming network was included. The signals from the whistler probe contain a large low frequency component.

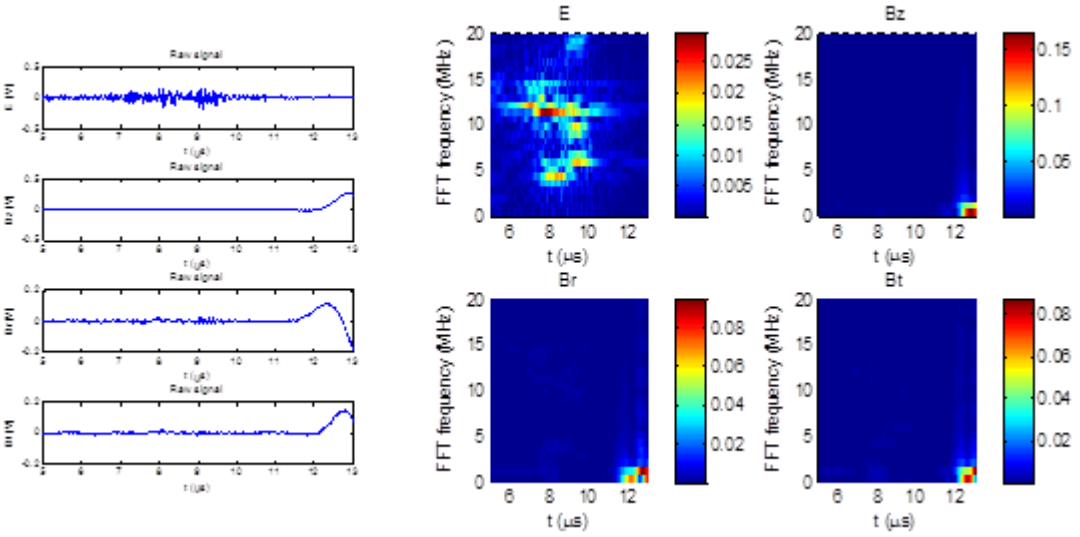

Figure 13: Shot #15139, CB+PFN. (left) plot of the signals over time for capacitive coupling probe and each of the channel of the whistler probe (right) the FFT of the graph on the left

4. Conclusion

The probe to detect a magnetic component of the whistler wave is made. It has a fast time respond (good up to 20 MHz). The capacitive coupling pickup signal is small comparing to the inductive signal and it can resolve the direction of the magnetic field in 3D (polarization property can be observed).

There are, however, few features that the probe can be improved. First, high-pass filter can be added before reading out the signal. The filter will allow high frequencies signal to pass so as to prevent the result in the last shot to occur again. Although the calibration test agrees well with the prediction, the probe can be recalibrated for more accuracy. So far, only Argon plasma was used in the shots. Other gases can be used as well.

5. Reference

[1] G. Paschmann et al. (1979). Plasma acceleration at the Earth's magnetopause: evidence for reconnection. *Nature 282*, 243-246.

[2] S. Colgate, H. Li, and V. Pariev. (2001). The origin of the magnetic fields of the universe: the plasma astrophysics of the free energy of the universe. *Phys. Plasma 8*, 2425-2431.

[3] Wesson, J. A. (1990). Sawtooth reconnection. *Nucl. Fusion 30*, 2545-2549.

[4] Auna L. Moser, and Paul M. Bellan. (2012). Magnetic reconnetion from a multiscale instability cascade. *Nature 482*, 379-381.

[5] Huddlestone, R. H. (1965). Magnetic Probes. In R. H. Lovberg, *Plasma Diagnostic Techniques, Vol. 21, Chap. 3* (pp. 69-112). New York: Academic.

[6] R. C. Phillips and E. B. Turner. (1965). Construction and Calibration Techniques of High Frequency Magnetic Probes. *Rev. Sci. Instrum. 36, 1822*, 1822-1825.

[7] Lochte-Holtgreven, W. (1968). *Plasma Diagnostics.* New York: American Institute of Physics.

[8] C. A. Romero-Talamás, P. M. Bellan, and S. C. Hsu. (2004). Multielement magnetic proe using commercial chip inductors. *Rev. of Sci. Instru. Vol. 75, no. 8*, 2664-2667.

[9] Moser, A. L. (2012). *Dynamics of magnetically driven plasma jets: An instability of an instability, gas cloud inpacts, shocks, and other deformations.* Pasadena, California: Unpublished doctoral dissertation, California Institute of Technology.

[10] Stenson, E. (2012). *Fields, forces, and flows: What laboratory experiements reveal about the dynamics of arched plasma structures.* Pasadena, California: Unpublished doctoral dissertation, California Institute of Technology.

[11] Helliwell, R. A. (1965). Whistlers and related ionospheric phenomena. *Standford University Press*.

[12] Stenzel, R. L. (1999). Whistler waves in space and laboratory plasmas. *Journal of Geophysical Research-Space Physics 104, 14379*.

[13] Michael p. Reilly, William Lewis, and George H. Miley. (2009). Magnetic field probes for use in radio frequency plasma. *Rev. Sci. Instrum. 80, 053508*.

[14] S. Messer, D. D. Blackwell, W. E. Amatucci, and D. N. Walker. (2006). Broadband calibration of radio-frequency magnetic induction probes. *Rev. Sci. Instrum. 77, 115104*.

[15] R. C. Phillips and E. B. Turner. (1965). Construction and Calibration Techniques of High Frequency Magnetic Probes. *Rev. Sci. Instrum. 36, 1822*, 1822-1825.